ENGINEERING TRANSACTIONS • *Engng. Trans.* • **45**, 3–4, 505–531, 1997
Polish Academy of Sciences • Institute of Fundamental Technological Research

MODELING OF SPALL FRACTURE IN BRITTLE SOLIDS(*)

M. BASISTA (WARSZAWA)

This is a synthetic and critical review of the selected theories of brittle spall fracture. Since the main body of research done on spalling can actually be credited to a few research institutions, the papers selected for this overview are classified according to their place of origin with some effort to maintain their order of appearance. Emphasis is placed on those models which were instrumental in the development of spall fracture modeling in brittle solids. Consequently, early models based on the critical stress criterion are merely recalled whereas micromechanical and phenomenological damage models of brittle spalling are discussed in more detail. The methods developed in the physics of critical phenomena (e.g. percolation theory), so far relatively unexplored in the modeling of dynamic fracture processes, are also outlined.

Specific Notation

D damage parameter (in general),
ω Walsh (Budiansky–O'Connell) crack density parameter,
ξ microvoid volume fraction (porosity).

1. Introduction

Dynamic failure processes are typically divided into three main classes, e.g. Zurek and Meyers [1]:

• dynamic failure in tension: uniaxial strain state (spalling) or uniaxial stress state; both metallic and brittle materials are prone to this mode of failure,

• dynamic failure in shear (shear band instability); exhibited by many metals and metallic alloys,

• dynamic failure in compression; important in rocks, ceramics and brittle metals subject to shock waves.

Spall fracture (spalling, spallation) is a specific type of dynamic fracture that results from the tensile stresses generated by the interaction of propagating waves of rarefaction. Spalling is produced by impulsive loads of high intensity and short duration times, such as projectile impact onto the surface of a target,

(*) A critical review.

air shock loading, explosions, etc. More specifically, in the case of plate (flyer) impact, the initial compressive wave traveling across the target reflects back at the free surface as a propagating decompression wave. A similar process, oppositely directed, occurs in the thinner flyer plate. The superposition of the reflected decompression wave fronts can cause partial and complete separation of the material along a plane perpendicular to the direction of the traveling wave fronts.

In general, the spall damage consists of the same basic phases as the static damage process, i.e. nucleation, growth and coalescence of microcracks or voids, whereas the overall failure is understood as a complete separation of a target into disjoint elements. However, unlike the static case, duration of a shock impulse is too short to allow for a long penetration of individual microcracks through large material areas. Also, crack interaction effects are not so pronounced. Instead, numerous microcracks (voids) nucleate, intersect and form complex clusters that transform into a dominant macrocrack or lead to material fragmentation.

One distinguishes ductile and brittle spall damage. Ductile spall damage assumes a form of small roughly spherical voids. Such voids are typically observed in copper, soft aluminum and tantalum. Brittle spall damage is associated with the development of planar microcracks. It occurs, for instance in ceramics, rocks, Armco iron, beryllium and polycarbonates. In one-dimensional wave propagation problems, the spall damage of either type usually occupies a major part of the target volume. As time elapses, the concentration of voids (cracks) gets denser in the narrow zones that are perpendicular to the impact direction and are localized near the target center. In ductile spalling, the voids enlarge, coalesce and create a macrocrack that runs through a heavily damaged material, leading finally to a full separation of the impacted specimen. A transition from ductile to brittle tensile fracture is possible at high strain rates since the yield stress is strain rate dependent. This kind of behavior is observed in steels if the shock pressure exceeds 13 GPa. This particular value of pressure is related to the reversible phase transformation in iron and steels.

In brittle solids, the process of fragmentation occurs as the microcracks link up. Fragments of various sizes are generated by the intersections of microcracks having different lengths. Since the fragmentation inevitably involves some empty spaces among the separated parts, the stress in the effective cross-sectional area must increase in order to sustain the external load. In turn, more and more microcracks get activated and new fragments are formed. The whole process reaches a self-accelerating cataclysmic stadium which ends by a complete material deterioration.

Spall damage has been a subject of intensive research for quite some time. The first experimental studies of the phenomenon are due to HOPKINSON [2] who

correctly identified spalling when gun-cotton was detonated in contact with mild steel plates. After World War II, the spall research was basically determined by the military purposes and concentrated in a few research centers. A pioneering, systematic spall-oriented experimental program was carried out by RINEHART [3, 4] on steel, brass, copper and aluminum. He proposed the first spall criterion stating that spall fracture occurs whenever the normal tensile stress carried by the reflected wave exceeds a critical value which is characteristic of the material. He also investigated and correctly described the so-called multiple spalling that occurs when a triangular pulse has an amplitude considerably higher than the critical spall stress. A decade later, Rinehart's simple spall criterion was proven insufficient because different values of the critical spall stress were obtained for different thicknesses of the same target material (e.g. SMITH [5]). A remedy for this unphysical prediction was sought in introducing into considerations the duration of tensile wave pulse, TULER and BUTCHER [6]. However, that could not improve the situation either, for the problem was of more fundamental nature. Both criteria entirely ignored the internal damage within the material, an important factor that influences the magnitude and the duration of tensile stress pulse. Therefore, not denying their merits in the historical development of constitutive theories of spall fracture, these models were later abandoned in the literature and will not be analyzed in detail in this paper either. It became evident, though, that some measure of microdamage and its evolution are necessary in order to capture the salient features of the material behavior at spall fracture.

The primary objective of this review is to give a synthetic and critical account of the existing theories of brittle spall fracture. In terms of the dynamic failure classification given at the beginning of this section, our objective here is confined to the brittle regime within the first class of failure processes. Obviously, the present study represents author's own, and rather biased views on spall modeling, and by no means it can be claimed complete. Extensive state-of-the-art papers by GRADY and KIPP [7], MEYERS [8], EFTIS [9] are recommended to gain a deeper insight into this intensively growing field of solid dynamics.

2. BRITTLE SPALL MODELING: SANDIA NATIONAL LABORATORIES

Even a cursory inspection of a vast body of the existing literature on spall fracture reveals the fact that research in this field concentrated mostly in several institutes and national laboratories in the United States. Although it may not be true now, it was undoubtedly the case in the seventies and the eighties. The spall research activities at Sandia National Laboratories, Stanford Research Institute, Los Alamos National Laboratory, Lawrence Livermore National Laboratory and

Dayton Research Institute laid down the foundations for the modern theories of spalling.

2.1. Davison and Stevens' models

As pointed out in the preceding section, at rapid loading rates a single crack with bounded growth velocity is not sufficient to relieve the increasing tensile stress. Other cracks, inherently present in brittle solids, get destabilized leading to a more continuous cracking patterns. Consequently, rather than the analysis of a single crack propagation, a concept of spall damage seems to be more descriptive of the spall fracture process. In continuum damage mechanics models, some measure of the internal material deterioration must be defined.

Davison and Stevens were first who introduced the concept of continuous spall damage. In their early paper (DAVISON and STEVENS [10]), the precise definition of "damage" has been left open. In the examples considered, the damage was described by a scalar parameter being the volume fraction of voids or fractional reduction in tensile strength across the spall plane. DAVISON and STEVENS' [10] damage model was phenomenological in the sense that no detailed mechanisms for initiation and growth of microflaws were offered. A year later, DAVISON and STEVENS [11] published an important paper where fundamental concepts necessary in a thermodynamically consistent continuum description of brittle spalling were established. The authors introduced the spall damage in terms of a vector field characterizing the size and spatial distribution of small penny-shaped cracks throughout the material volume. The crack was assumed to be fully characterized by its position, orientation and area. In the reference configuration, all these information of the crack at the material point $\mathbf{X}$ and time t were stored in a vector $\mathbf{D}(\mathbf{X}, t)$ normal to the plane of the crack and having the magnitude equal to the crack area. In the actual configuration, $\mathbf{D}(\mathbf{X}, t)$ is transformed into $\mathbf{d}(\mathbf{x}, t)$ since the crack is convected along with the body motion. The vectorial damage parameters $\mathbf{D}$ and $\mathbf{d}$ were regarded as continuum field variables (internal state variables) defined over the entire body instead of at isolated cracks. In other words, the orientations of these vectors represented the average orientation of cracks in the neighborhood of the considered material point, whereas their lengths – the averaged projected area fraction of the material that is cracked. The damage was allowed to occur gradually according to some specified damage accumulation equation. The model was then completed by theoretical considerations of the interaction between propagating waves and the accumulating damage. However, numerical implementations of the theory into the existing wave propagation codes were not yet given. Note that this theory was devised to describe brittle spalling in the thermoelastic materials.

Further extension of the above concepts to account for ductile spalling was developed by DAVISON, STEVENS and KIPP [12]. The mechanical response of the material was assumed to be viscoplastic. Based on the experimental evidence of SEAMAN, BARBEE and CURRAN [13], the spall damage was modeled by small spherical voids diffusely distributed over the material volume. Mathematically, it can be represented by a scalar function $\xi(\mathbf{X}, t)$, the void volume fraction (porosity). The number density of voids in very ductile metals is typically of the order of $10^4/\text{mm}^3$ whereas the void average volume can be estimated at $10^{-6}\,\text{mm}^3$. The central assumption of the constitutive framework in [12] was that the deformation gradient tensor $\mathbf{F}$ can be decomposed as

$$\mathbf{F} = \mathbf{F^e} \cdot \mathbf{M} \cdot \mathbf{F^p}, \tag{2.1}$$

where $\mathbf{F^p}$ is associated with viscoplastic flow, $\mathbf{F^e}$ with thermoelastic deformation, $\mathbf{M}$ represents spall dilatation being related to ξ by

$$\mathbf{M} = \left(\frac{1}{1-\xi}\right)^{1/3} \mathbf{1} = M\mathbf{1}. \tag{2.2}$$

The constitutive equation for viscoplastic response is modeled in terms of a dislocation theory of plasticity. As for the reversible part of deformation, it is assumed that the solid be thermoelastic and deformations remain small.

The evolution equation for porosity is obtained by postulating evolution equations for the number of voids per unit volume N and for the average void volume V. Introducing some additional assumptions to preclude pore collapse to volumes less than V_0, and performing simple algebraic manipulations, the final form reads

$$\dot{\xi} = \left(fV_0 + 3A'\frac{\xi}{1-\xi}\right)(1-\xi)^2, \tag{2.3}$$

where the material functions f and A' that depend on the hydrostatic stress and temperature, must be determined experimentally. A few numerical examples of spallation in plate impact tests for aluminum and copper were computed to verify the proposed theory. In doing so, the authors incorporated their model into a one-dimensional Lagrangian wave propagation code using the finite difference method (WONDY code). The comparison showed a very good agreement with the appropriate experimental data.

2.2. Grady's models

The processes of spall fracture and fragmentation in rocks have found the most elaborated mathematical description in the papers by GRADY and KIPP [14, 7], and GRADY [15, 16].

A brittle rock contains a certain initial distribution of cracks which can be thought of as a material property. Under the action of dynamic tensile loading, some of these cracks get activated, grow and intersect one another to form fragments of different sizes. GRADY and KIPP [14] characterized the tensile fracture in rocks by a scalar parameter D specified as follows

$$D = NV, \tag{2.4}$$

where N is the number of penny-shaped cracks per unit volume, $V = (4/3)\pi r^3$ is a spherical volume surrounding the crack of radius r. This volume approximates the stress-relieved region in the vicinity of the traction-free crack surfaces. The concept of a stress-relieved volume in the continuum description of damage was originally introduced by WALSH [17] in an approximate micromechanical theory of the effective elastic properties of rocks. The scalar damage parameter (2.4) takes the values

$$0 \leq D \leq 1, \tag{2.5}$$

such that $D = 0$ corresponds to an intact rock, whereas $D = 1$ represents the final failure (fragmentation). Macroscopically, the damage D can be seen as the reduction of the elastic modulus of a damaging material in a uniaxial tension. Therefore, a one-dimensional stress-strain relation can be written as

$$\sigma = E(1 - D)\varepsilon, \tag{2.6}$$

where E is the intrinsic elastic modulus of the material. Equations (2.5) and (2.6) were among the first ideas promoted in the seventies in the early papers on continuum damage mechanics (see, for example, LEMAITRE and CHABOCHE [18]).

A dimensional analysis of "crack energy" in BUDIANSKY and O'CONNELL [19] involves, in a natural way, a crack density parameter ω given by

$$\omega = N\langle r\rangle^3, \tag{2.7}$$

where N, as before, denotes the crack number density, $\langle r\rangle$ is the average radius of a penny-shaped crack. In a two-dimensional case, a penny-shaped crack degenerates to a slit, and (2.7) reduces to $\omega = N\langle r\rangle^2$. Note that the crack density parameter (2.7) appeared earlier in WALSH [17].

According to GRADY and KIPP [14], the accumulated damage at time t in the dynamic case is the superposition of the stress-relieved spherical volumes of all penny-shaped cracks which were activated at past times τ. Therefore, using (2.4) one gets

$$D(t) = \int_0^t \dot{N}(\tau)V(t - \tau)\, d\tau\,, \tag{2.8}$$

where $\dot{N}$ is the rate of crack activation, $V(t-\tau)$ is the stress-relieved volume around the crack activated at time τ. In (2.8), an assumption is hidden that in the stress-relieved region no subsequent crack activation is allowed. The authors further assume that crack activation is governed by a two-parameter Weibull distribution

$$n = k\varepsilon^m, \tag{2.9}$$

where n is the number of flaws which will activate at or below a tensile strain level ε; k and m are material constants characterizing fracture activation. Since the cracks will actually activate in the material outside the stress-relieved regions, the number of such cracks must be reduced by a factor of $(1-D)$. Hence, the rate of crack activation becomes

$$\dot{N} = n'(\varepsilon)\dot{\varepsilon}(1-D) = km\varepsilon^{m-1}\dot{\varepsilon}(1-D). \tag{2.10}$$

The volume of a stress-relieved region V is calculated assuming that cracks, once activated, quickly approach a constant growth velocity c_g, which is treated as an additional fracture property of the material. Consequently, the authors claim that

$$V(t-\tau) = \frac{4}{3}\pi c_g^3 (t-\tau)^3, \tag{2.11}$$

where it was tacitly assumed that initial crack radius is negligibly small. Finally, the following integral equation is obtained for the damage D

$$D(t) = \frac{4}{3}\pi c_g^3 \int_0^t n'(\varepsilon)\dot{\varepsilon}(1-D)(t-\tau)^3\, d\tau, \tag{2.12}_1$$

or, upon inserting the rate of flaw activation based on the Weibull distribution (2.10),

$$D(t) = \frac{4}{3}\pi km c_g^3 \int_0^t \varepsilon^{m-1}\dot{\varepsilon}(1-D)(t-\tau)^3\, d\tau. \tag{2.12}_2$$

GRADY and KIPP [14] further specialized equation $(2.12)_2$ for a *constant* strain rate $\varepsilon(t) = \dot{\varepsilon}_0 t$. Hence,

$$D(t) = \frac{4}{3}\pi km c_g^3 \dot{\varepsilon}_0^m \int_0^t \tau^{m-1}[1-D(\tau)](t-\tau)^3\, d\tau. \tag{2.13}$$

Clearly, this assumption is a restriction of the presented theory. On the other hand, it may be justified by the fact that it admits a closed-form, though approximate, solution which facilitates interpretation of the theory. It is also convenient when designing an experimental program to verify the obtained theoretical results. Solving Eq. (2.13) by a series expansion and neglecting the higher order terms, the authors obtained that

$$D(t) = \alpha \dot{\varepsilon}_0^m t^{m+3}, \tag{2.14}$$

where

$$\alpha = \frac{8\pi k c_g^3}{(m+1)(m+2)(m+3)} \tag{2.15}$$

is a combined constant involving three material fracture parameters k, m, c_g. Inserting the solution (2.14) into the stress-strain equation (2.6) gives

$$\sigma(t) = E\dot{\varepsilon}_0 t \left(1 - \alpha \dot{\varepsilon}_0^m t^{m+3}\right). \tag{2.16}$$

The dynamic fracture stress, defined as the highest stress in the material prior to failure, is obtained from (2.16) by maximizing it with respect to time:

$$\sigma_c = E(m+3)(m+4)^{-(m+4)/(m+3)} \alpha^{-1/(m+3)} \dot{\varepsilon}_0^{3/(m+3)}. \tag{2.17}$$

The fracture stress (2.17) is reached at the time

$$t_c = (m+4)^{-1/(m+3)} \alpha^{-1/(m+3)} \dot{\varepsilon}_0^{-m/(m+3)}. \tag{2.18}$$

To make a brittle spall model complete, a fragmentation criterion is necessary. GRADY and KIPP [14] postulated that fragmentation occurs when their scalar damage variable reaches the upper limit, i.e.

$$D(t_f) \equiv 1. \tag{2.19}$$

This is expected to happen at a time t_f (time to fragmentation) when coalescing cracks form such a pattern that the material is no more able to transmit tensile stresses. The time to fragmentation is computed from Eq. (2.14) on which the side condition (2.19) is imposed. The mean fragment size is then approximated to be $L_f = c_g t_f$. Performing a somewhat more detailed analysis of crack size distribution, GRADY and KIPP [14] obtained, in the constant strain-rate case, the following mean fragment size:

$$L_f = \frac{6c_g}{m+2} \alpha^{-1/(m+3)} \dot{\varepsilon}_0^{-m/(m+3)}, \tag{2.20}$$

where, again, three fracture parameters c_g, m, k are involved. The three fracture constants c_g, m, k are difficult to obtain from direct experiments. Instead, they were inferred from the test data by the best fitting. Material properties such as the fracture stress and fragment size were measured for different loading rates and intensities using several experimental methods. These included: a gas gun impact technique, a capacitor discharge technique, explosions in cylindrical samples, a split Hopkinson bar method. The rock under investigation was an oil shale from Colorado for which a vast body of the above data existed. Using the obtained experimental data regarding the fracture stress vs. strain rate, GRADY and KIPP [14] performed a linear fitting using Eq. (2.17). From the slope and the intercept of that linear fit they determined the fracture parameters. For the oil shale they obtained $m = 8$ and $\alpha = 9.48 \cdot 10^{34}$. The strain-rate dependence of the fracture stress was found to be $\sigma_c \propto \dot{\varepsilon}_0^{0.27}$. However, the separate fracture parameters k and c_g could not be singled out using the fracture stress data only. In order to do that, additional experimental data concerning the nominal fragment size vs. strain rate were needed. Using the fragmentation data for the Colorado oil shale, a value for the crack growth velocity of $c_g = 1300\,\mathrm{m/s}$ was obtained. This is about 0.4 of the longitudinal wave velocity – a reasonable upper bound for the fracture velocity.

Before closing the discussion of the GRADY and KIPP'S [14] model, the following point should be addressed. In addition to the integral equation $(2.12)_1$ from which the damage parameter D is to be determined, the authors give a following rate equation:

$$\dot{D} = \left[\frac{8\pi(m+3)^2}{(m+1)(m+2)}\right]^{1/3} C_g n(\varepsilon)^{1/3} D^{2/3}, \tag{2.21}$$

which has an advantage of being computationally simpler. They claim that (2.21) is derivable from $(2.12)_1$, and for the particular case of a constant strain-rate loading it agrees exactly with the integral equation (2.13). The first statement is not straightforward to verify. As far as the second one is concerned, the differential equation (2.21) can be integrated directly giving

$$D(t) = \frac{8\pi k c_g^3}{(m+1)(m+2)(m+3)} \dot{\varepsilon}_0^m t^{m+3}. \tag{2.22}$$

Surprisingly, this solution is identical to the expression (2.14) obtained in GRADY and KIPP [14] by a series expansion under the assumption that higher order terms be neglected. This is rather unexpected since no assumption regarding higher order terms was declared when arriving at Eq. (2.21). However, when $D(\tau)$ from (2.22) is inserted into the integral equation (2.13), it turns out that (2.13) is

not satisfied identically. The only case when the expression (2.22) becomes a solution for (2.13) is when the term $[1 - D(\tau)]$ in (2.13) is set equal to 1. Recall that $[1 - D(\tau)]$ is a factor that reduces the number of activated cracks as the damage proliferates within the material volume. Setting $D(\tau) = 0$ in Eq. (2.13) physically means that an apparent decrease of the number of activated cracks as the undamaged volume shrinks, is counter-balanced by a possible increase of the number of activated cracks in the remaining undamaged volume. A plausible explanation of this scenario may be related to the fact that higher stress levels and crack interaction effects may amplify the crack activation rate. In such circumstances, the integral equation (2.13) reduces to a determined integral and the above indicated inconsistency vanishes. Note also that this is equivalent to what GRADY and KIPP [14] did when they neglected the higher order terms in their series solution to Eq. (2.13). The influence of those higher order terms was estimated to be less than 5%, even at the overall damage levels close to 1.

Another shortcoming of the GRADY and KIPP'S [14] model is that the underlying energetic background of the brittle spallation was entirely ignored. This aspect was later addressed by GRADY [15], and refined in [16]. Claiming that primitive spall properties such as spall strength, time to failure, and nominal fragment size are less sensitive to microstructural details of the material, Grady concentrated on the energy balance analysis involving the elastic strain energy, the kinetic energy, and the fracture surface energy, in order to assess the theoretical values of these properties at brittle spall. For a brittle spall to be energetically permissible, the fracture driving energies (the kinetic energy due to volumetric expansion and the elastic stored energy) within an element of mass δM must overcome the resistance of the material, i.e. exceed its fracture surface energy

$$U + T \geq \Gamma, \tag{2.23}$$

where U, T, Γ denote the elastic-, local kinetic-, and fracture surface-energy density, respectively. The individual terms in (2.23) are given by:

$$U = \frac{1}{2}\frac{P^2}{\varrho c_0^2}, \qquad T = \frac{1}{120}\varrho \dot{\varepsilon}^2 s^2, \qquad \Gamma = \frac{3K_{Ic}^2}{\varrho c_0^2 s}, \tag{2.24}$$

where P is the mean tension stress within an expanding elastic body, ϱ is the mass density, c_0 is the sound speed, s is an average fragment size, $\dot{\varepsilon} = -\dot{\varrho}/\varrho$ is the dilational strain rate (assumed constant), K_{Ic} is the fracture toughness.

The mean tension in the expanding body is related to the time according to

$$P = \varrho c_0^2 \dot{\varepsilon} t, \tag{2.25}$$

where $\varrho c_0^2 = B_0$, with B_0 being the bulk modulus of the material. Assuming, for simplicity, that cracks propagate from the sites of a rectangular lattice, the

nominal fragment size was deduced to obey the following inequality

$$s \leq 2c_0 t\,. \tag{2.26}$$

To compute the minimum time to fracture, the criteria (2.24) and (2.26) were taken in their equality forms. Combined with Eq. (2.25), they were solved for the three primitive spall properties in question, giving

$$P_s = \sqrt[3]{3\varrho c_0 K_{Ic}^2 \dot{\varepsilon}} \qquad \text{(brittle spall strength)}, \tag{2.27}$$

$$t_s = \frac{1}{c_0}\sqrt[3]{\frac{3K_{Ic}^2}{(\varrho c_0 \dot{\varepsilon})^2}} \qquad \text{(time to spall fracture)}, \tag{2.28}$$

$$s = 2\sqrt[3]{\frac{3K_{Ic}^2}{(\varrho c_0 \dot{\varepsilon})^2}} \qquad \text{(mean fragment size)}. \tag{2.29}$$

The contribution of the kinetic energy in (2.24) was found to be small as compared with the elastic stored energy, and was neglected in the above computations. Incidentally, in an earlier paper (GRADY [15]) it was the kinetic energy that was neglected in the energy balance equation (2.23). The utility of the model predictions (2.27), (2.28), (2.29) was assessed in [16] by confronting them with the extensive impact spall data on rock materials. The calculated spall strength, time to failure, and mean fragment size were generally consistent with the experimental evidence.

A similar analysis was performed in [16] for ductile spall. The differences in ductile and brittle spall are due to different mechanisms of energy dissipation. The most part of the fracture energy in a ductile spall results from the local plastic dissipation during void growth. Unlike the brittle case, the surface energy of newly created voids is negligible in comparison with the plastic dissipation. To estimate the energy dissipated in ductile spall, Grady relied on the Gurson's model [20] of a spherical cavity growth in a rigid-plastic solid, with the subsequent modifications by TVERGAARD and NEEDLEMAN [21]. In a recent study [22], Grady extended the above outlined energetic theory of spall fracture to account for the influence of temperature on spall and fragmentation in solid and liquid metals.

Grady's energetic approach to spall fracture may be summarized as follows. Although the need for microscopic studies of spall fracture cannot be overemphasized, it is likewise important to investigate the primitive spall properties (2.27), (2.28), (2.29). These properties might be less sensitive to microstructural details, depending more on the driving and opposing energies during the transcient wave loading. Continuum energy concepts provide bounds on the micromechanical theories of nucleation and growth of spall fracture.

3. Stanford Research Institute

The names of L. Seaman, D.R. Curran and D.A. Shockey, in all possible permutations, are usually encountered when referring to spall damage investigations at the Stanford Research Institute (SRI). Their research work was basically concerned with modeling the nucleation and growth of microvoids and microcracks in damaged solids. They also performed experiments and collected systematic statistical measurements of defect size distributions at different stages of spall damage development. This data was then employed to establish nucleation and growth rate equations for spallation in ductile and brittle solids for a variety of loading conditions.

In the classical paper of Seaman, Curran and Shockey [23], computational models were formulated for both ductile and brittle dynamic fracture, and implemented in one- and two-dimensional wave propagation problems. Although the primary objective of this review is the brittle spall, we shall briefly outline the Seaman *et al.* [23] model of ductile spall because their brittle part utilizes the same basic concepts. From the observations of the polished cross-sections of copper and aluminum targets after impacts, these authors concluded that the number density of nearly spherical voids can be approximated with a sufficient accuracy by the following expression

$$N(R) = N_0 e^{-(R/R_N)}, \tag{3.1}$$

where N is the cumulative number of voids (per unit volume) having radii larger than R, N_0 is the total number of voids per unit volume, R_N is a parameter of the distribution. The total void volume follows from the integration over the entire distribution assumed to be spherical in shape

$$V_{\text{void}} = \int_0^{N_0} N(R)\, dN = (4/3)\pi \int_0^{\infty} R^3 \frac{dN}{dR}\, dR = 8\pi N_0 R_N^3 . \tag{3.2}$$

Nucleation of new voids with a size distribution defined by (3.1), occurs at a rate given by

$$\dot{N} = \dot{N}_0 e^{(\sigma_s - \sigma_n)/\sigma_1}, \qquad \text{for} \quad \sigma_s > \sigma_n , \tag{3.3}$$

where σ_n is the nucleation threshold, σ_s is the tensile pressure in the solid material, $\dot{N}_0$ is the nucleation rate at σ_n, σ_1 is an additional material constant, the dot denotes time derivative. The growth of the existing voids is assumed to proceed at the following rate:

$$\dot{R} = \frac{1}{4\eta}(\sigma_s - \sigma_g) R , \tag{3.4}$$

where σ_g is the growth threshold stress, η is the material viscosity. The total change in void volume comprises the contributions due to nucleation and growth alike. Therefore, integrating (3.3) and (3.4) for the time interval Δt, and inserting the results into (3.2) gives

$$V_{\text{void}} = 8\pi N_0 R_N^3 e^{(\sigma_s - \sigma_n)/\sigma_1} \Delta t + V_{t0} e^{(3/4\eta)(\sigma_s - \sigma_g)\Delta t}, \tag{3.5}$$

where V_{t0} is the void volume at the beginning of the time interval Δt, and $R_N = R_n$ at nucleation, with R_n being the nucleation size parameter. Having quantified the nucleation and growth of voids, the constitutive equations accounting for the presence of voids were formulated for the volumetric and deviatoric parts of the stress tensor. Without going into the details of these stress-strain relations, it suffices to say that they were successfully implemented in the stress wave numerical codes to account for ductile spall fracture in aluminum and copper.

A brittle spall model in [23] was formulated on the basis of a careful microscopic inspection of the fractured targets made of Armco iron, beryllium and transparent plastics, where the primary damage mode appears as cracks. Unlike the ductile spalling where spherical voids were dominant, in modeling brittle spall damage both the size and orientation distributions of cracks are of importance. From the target observations, surface distributions of crack sizes and orientations were constructed, and then transformed statistically into three-dimensional distributions of idealized penny-shaped cracks. Based on these observations, a relation similar to (3.1) was assumed for the cumulative crack density in brittle solids:

$$N^{ij}(R) = N_0^{ij} e^{-(R/R_1^{ij})}, \tag{3.6}$$

where the indices i and j uniquely designate a spherical surface element in the array of orientations distribution, N_0^{ij} is the number density of cracks contained in the ij-th element, and R_1^{ij} is a shape parameter of the ij-th element. Only Mode I penny-shaped cracks with no plastic zones around crack perimeter were considered. Thus, assuming that a penny-shaped crack, when opened, forms an ellipsoid with the semi-axes R, R, δ, the elastic opening δ is given by a familiar formula:

$$\delta_{ij} = \frac{4(1-v^2)}{\pi E} R \sigma_{\varphi\psi}^{ij}, \tag{3.7}$$

where $\sigma_{\varphi\psi}^{ij}$ is the normal stress acting on a crack with angular coordinates φ_i and ψ_j. Computing the volume of a single crack, and combining it with the cumulative crack concentration (3.6), the ensuing total volume of the crack distribution becomes

$$V = \frac{32(1-v^2)}{E} \sum_{i,j} N_0^{ij} (R_1^{ij})^3 \sigma_{\varphi\psi}^{ij}. \tag{3.8}$$

Nucleation of new cracks and growth of the existing set were considered next. Similarly to what the authors did for ductile spall, the nucleation rate in the brittle case is governed by

$$\dot{N}^{ij} = \dot{N}_0^{ij} e^{(\sigma_{\varphi\psi} - \sigma_{n0})/\sigma_1}, \tag{3.9}$$

where $\dot{N}_0$, σ_{n0}, σ_1 are fracture parameters. On the basis of (3.8), the entire volume of newly nucleated cracks follows to be

$$V_n = \frac{32(1-v^2)}{E} \sum_{ij} \dot{N}^{ij} \Delta t R_n^3 \sigma_{\varphi\psi}^{ij}, \tag{3.10}$$

where $\dot{N}^{ij}\Delta t$ gives the total number of cracks nucleated in the ij-th element within the time step Δt, R_n is the nucleation distribution parameter. The rate equation for crack growth deduced from the experimental data has the same functional form as in the ductile case

$$\dot{R} = G_1(\sigma - \sigma_{g0})R, \tag{3.11}$$

where G_1 is a growth coefficient, σ_{g0} is the growth threshold stress assumed constant for impact problems. Integrating (3.11) over a time step Δt yields the final crack size

$$R = R_1 e^{G_1(\overline{\sigma}_{\varphi\psi} - \sigma_{g0})\Delta t}, \tag{3.12}$$

where R_1 is the initial crack radius, and $\overline{\sigma}_{\varphi\psi}$ the average stress in the Δt interval. The crack volume associated with the growth is obtained from (3.8) and (3.12), as

$$V_g^{ij} = \frac{32(1-v^2)}{E} N_0^{ij} (R_1^{ij})^3 \sigma_{\varphi\psi}^{ij} e^{3G_1(\overline{\sigma}_{\varphi\psi}^{ij} - \sigma_{g0})\Delta t}. \tag{3.13}$$

The total number of cracks contained in the ij-th surface element at the end of Δt, reads

$$N_t^{ij} = N_0^{ij} + \dot{N}_g^{ij} \Delta t, \tag{3.14}$$

whereas the corresponding total crack volume is simply

$$V_t^{ij} = V_n^{ij} + V_g^{ij}, \tag{3.15}$$

with the individual terms given by (3.10) and (3.13).

A model for fragmentation in [23] makes use of a string of experimental facts. For example, it has been observed in rocks and brittle metals that fragments are usually chunky objects having six to eight sides, each of which being probably generated by one crack. Consequently, the number of cracks involved in

the fragmentation may be estimated from the number of fragments. Also, each large fragment contains quite a lot of tiny cracks that do not participate in the fragment formation. Finally, the fragment-size distributions exhibit similarity to the crack-size distributions, thus they can be approximated by the same distribution function (3.6). The fragment volume is represented as $T_f R_f^3$, where the proportionality factor T_f depends on the shape of the fragment. A criterion for fragmentation is based upon the concept of a crack range $V_{\rm cr}$. Roughly speaking, $V_{\rm cr}$ is defined as the volume surrounding a crack that experiences magnified strains due to stress concentrating effect of the crack (SHOCKEY *et al.* [24]). Once the crack ranges of two cracks intersect, the cracks interact strongly. Unfortunately, the authors did not offer a precise definition of $V_{\rm cr}$ except for stating that it is a sole function of the crack size. Therefore,

$$V_{\rm cr} = T_c R^3, \tag{3.16}$$

where T_c is a material constant which may range from 1 for very ductile materials, to much higher values for very brittle ones. The crack range concept bears some resemblance to the excluded volume concept in the percolation theory (cf. Sec. 6), and plays a similar role as Grady and Kipp's stress relieved region (cf. Subsec. 2.2). The onset of fragmentation is controlled by the condition $V_{\rm cr} = 1$.

The theoretical spall model by SEAMAN *et al.* [23] was thoroughly tested against exhaustive data obtained by the authors from tapered-flyer impact experiments on brittle and ductile targets. The comparison of the predicted and measured damage distributions, void and crack concentrations, cumulative number of fragments, showed fairly good agreement for various materials, impulse intensities and load duration. In conclusion, this is a workable computational model of spall fracture that is firmly rooted in the experimental evidence and contains a dependence on microstructural parameters. Its efficiency and tractability, though, is sometimes traded against mathematical rigor. Nevertheless, it is often recalled as one of the important models that gave rise to numerous extensions and improvements (e.g. GRADY and KIPP [14], PERZYNA [25]).

During the next 20 years, the SRI group established a family of computational models for spall fracture and fragmentation. These models were given a generic name of NAG/FRAG, for *Nucleation And Growth of damage to FRAGmentation* (CURRAN and SEAMAN [26]). The NAG/FRAG family has the following members: SHEAR for shear banding, BFRACT for brittle cracking (see CURRAN *et al.* [27] for details), DFRACT for ductile void growth, and FRAGBED for penetration of granulated materials (CURRAN *et al.* [28]). The common feature of all family members is that they require a laboratory-generated input data for the nucleation- and the growth rate equations of the intrinsic flaws in the material. The SRI group was able to develop effective techniques for measurements

of crack orientations, lengths, and numbers on a polished specimen's surface, and transform them to true orientations, lengths and numbers required in the NAG/FRAG computer codes.

4. Dayton Research Institute

The impact behavior of glass and ceramic materials was investigated by Rajendran, Bless and coworkers (see Bless and Rajendran [29], and references contained therein). These authors modeled the whole spectrum of impact-induced fracture phenomena such as nucleation, growth and coalescence of microcracks (damage), dynamic propagation of a macrocrack, and failure by moving fracture front. For ceramics, it is often assumed that intrinsic microcracks exist within the material prior to any impulse loading, thus nucleation process is not considered in the modeling. Typical features of spall damage in ceramics are: stiffness loss, small inelastic strains resulting from microcracking and from the microplastic zones due to dislocation motions in the neighborhood of the microcrack tips.

The total strain is typically decomposed into elastic and plastic portions

$$\varepsilon_{ij} = M_{ijkl}(\omega)\sigma_{kl} + \varepsilon^p_{ij}\,, \tag{4.1}$$

where M_{ijkl} is the effective compliance tensor, $\omega = N_0 a^3$ is the crack density parameter with N_0 being the average number of pre-existing cracks per unit volume, and a the maximum microcrack size. The proposed dynamic damage model is very simple. The pre-existing cracks extend independently from each other, according to Griffith criterion generalized for a dynamic case. The crack density parameter ω is treated as an internal state variable whose evolution depends only on the increase in crack length. Two material constants are involved: N_0 and a_0 which must be provided from experiments. The evolution law for $\omega = N_0 a^3$ follows from the crack stability condition for a dynamic Griffith crack, i.e.,

$$\dot{\omega} = 3n\frac{\omega}{a}C_R(1 - G_c/G), \tag{4.2}$$

where G_c is the critical strain energy release rate (related to fracture toughness), G is the actual strain energy release rate (related to dynamic stress intensity factors), C_R is the Raleyigh wave speed, and $n \leq 1$ is a parameter that puts bounds on the crack growth rate. Rajendran [30] assumed that at $\omega = 0.75$ the microcracks have reached the coalescence stage leading to disintegration of the ceramic. Rajendran *et al.* [31] developed also a constitutive-damage model for spallation in ductile materials.

5. Other models

Meyers with coworkers (Aimone *et al.* [32], Louro and Meyers [33], Meyers [8]) studied experimentally and theoretically the brittle spall damage and fragmentation in rocks and ceramics. They made an interesting observation that only a small fraction (ca. 15%) of the total energy expended during fragmentation is actually consumed in the creation and acceleration of the fragments. The remaining part of the blast energy was spent on producing microcracks contained within fragments. The measured surface area of those microcracks substantially exceeded the external surface area of the fragments. Consequently, it was concluded that "most of the damage is in the form of contained cracks, and the fragment size is not really a good measure of the damage produced" (Meyers [8]). Another important observation was that compressive pulse in the plate impact experiments creates crack initiation sites that may accelerate damage caused by the reflected tensile wave. Such compression-induced mechanisms of tensile cracking are well known in the literature of static crack growth (e.g. sliding crack mechanism, or squeezed pore mechanisms). Louro and Meyers [33] showed experimentally that less damage is produced if a tensile stress pulse runs through an intact material than if the material was previously subject to a shock (compressive) wave. Unlike the static crack growth in compression (cf. experiments by Horii and Nemat-Nasser [34]), the microcracks loaded by a shock wave do not seem to develop wings but they rather tend to grow in their own planes (self-similar growth), Dienes [35]. Another argument supporting the in-plane crack growth in dynamic tests is related to the strain rate level. High strain rates seem to favor nearly hydrostatic stress states. In hydrostatic stress states, the cracks grow in a self-similar mode, as noted by Horii and Nemat-Nasser [34]. At low strain rates, on the other hand, a tendency for wings to form prevails, Kalthoff and Winkler [36]. Based on the above observations, Louro and Meyers [33] formulated a theoretical model for spall damage and fragmentation in ceramics. They assumed that damage develops from the pre-existing microcracks as the shock wave travels across the material. The microcracks become larger but remain in their own planes. Then, a tensile wave makes them grow (again in their own planes) at a rate predicted by the fracture dynamics, i.e. less than the Rayleigh wave speed. Other cracks, which were not activated by the shock impulse, may also get moved by the tensile impulse and contribute to the increasing damage. The growing cracks form a complex pattern of straight lines that create fragments upon intersecting. The sizes of these fragments can be computed from the model. Noteworthy, Louro and Meyers incorporated, under the name of "shielding factor", the Walsh [17] concept of an unloaded region around a crack.

Ductile spall models were beyond the scope of this review. They were recalled only sporadically if a ductile spall model was helpful in explaining its brittle counterpart (vide the SRI models). For the sake of completeness, however, a few newer works on ductile spall will now be mentioned. JOHNSON [37] proposed a model for microvoid evolution due to tensile mean stress and used the derived equations to describe the ductile spall in impacted copper plates. Based on the pioneering work by SEAMAN *et al.* [23] and its subsequent modification by PERZYNA [25], EFTIS and NEMES [38] used a hollow sphere model to calculate the rate of increase of the void volume fraction. KLEPACZKO [39] proposed a cumulative spall criterion making use of the Boltzmann statistics and verified it experimentally for some aluminum alloys in plate impact tests.

A state-of-the-art in modeling of adiabatic shear banding is given in ZUREK and MEYERS [1], where an exhaustive list of references is also appended. As for the dynamic fracture under shock wave loading (compressive stresses), the research in this field is still in an adolescent phase. Some initial efforts based on the static micromechanics of local tensile cracking under overall compression are due to DENG and NEMAT-NASSER [40] and MEYERS [41].

The dynamic failure research in the countries of the former Soviet Union concentrated mostly on the penetration mechanics and fracture front propagation in impact phenomena (e.g. CHEREPANOV [42], NIKOLAEVSKI [43], ZILBERBRAND *et al.* [44], KANEL *et al.* [45].

6. PERCOLATION MODELS

Quite independently of the research conducted by the continuum mechanics community, brittle fracture processes are also investigated by statistical physicists who use an entirely different methodology. Instead of analyzing stress fields at the crack tips (fracture mechanics) or introducing *a priori* damage variables into a continuum constitutive description (damage mechanics), they simulate continuous brittle matter by means of discrete (regular or random) lattices which are subject to initial quenched disorder. The essential feature of the representation of a solid by a discrete graph is that it provides an opportunity to model the inhomogeneity of the microstructure by assigning appropriate statistical properties to the lattice bonds. The disorder can be introduced, for example, into elastic constants or into fracture thresholds of individual lattice elements. Out of several theoretical techniques available for dealing with the highly disordered systems, the percolation model seems to be particularly appealing. The intellectual advantage of the percolation model resides in its almost game-like mathematical structure, and in the fact that it provides a transparent and intuitively satisfy-

ing description for spatially random processes. Succinctly stated, the percolation disorder is bi-modal in the sense that a defect either occupies a considered site (or bond) of a lattice with a probability p or is absent there with the probability $1-p$. As the bonds start to break under external tensile loading, the spatial patterns of defects (clusters) and their sequence of appearance are believed to mimic a real breaking process. The central questions that are posed in the percolation and other statistical theories of disordered solids, are:

- What is the critical defect concentration p_c at which an infinite cluster appears spanning the opposite sides of the specimen (*percolation threshold*)?
- How do different processes and transport properties of the material behave in the vicinity of the percolation thresholds (*scaling laws*)? Is there any universal law that is common to all initial defect distributions? Does the total number of ruptured bonds at the overall failure and the maximum stress follow any universal law?

To get a deeper insight into the lattice modeling of disordered systems, the excellent monographs by ZALLEN [46], STAUFFER [47], HERRMANN and ROUX [48] should be consulted. Some specific conclusions concerning the links between the lattice models and the continuum damage mechanics were formulated in BASISTA and KRAJCINOVIC [49], KRAJCINOVIC *et al.* [50], KRAJCINOVIC [51]. The latter provides also an exhaustive list of original papers on statistical physics modeling of brittle fracture.

In the present section, we shall focus only on those aspects of the percolation theory that may have effect on the modeling of spall fracture. When examining the existing literature on applications of the percolation theory to brittle fracture modeling and confronting it with the damage mechanics findings, several interesting observations can be made.

An crack density parameter identical to that of Walsh - Budiansky - O'Connell (2.7) also appears in the percolation models. However, its genesis is different from that of (2.7). It was shown by SHER and ZALLEN [52] that the critical volume fraction of spherical or circular hard-core (non-overlapping) voids at percolation is a dimensional invariant independent of the lattice type. To visualize this statement, consider a simple case of circular voids whose centers are randomly located on the nodes of a regular two-dimensional lattice. The critical void surface area f_c can be determined directly using a site percolation model

$$f_c = p_c^s v \,, \tag{6.1}$$

where p_c^s is the site percolation threshold, v is the filling (packing) factor for the considered lattice. The percolation threshold p_c^s denotes the critical fraction of sites occupied by voids at the moment when an infinite void cluster transects a

two-dimensional specimen. Consequently, the equality (6.1) can be rewritten as

$$f_c = (NA_{\text{void}})_c \,. \tag{6.2}$$

According to SHER and ZALLEN [52], f_c was found to be equal to 0.45 ± 0.03 irrespective of the lattice type (Table 1). Moreover, the critical porosity f_c does not depend on the void shape. A similar universality of f_c was also confirmed for a bond percolation model (ZALLEN [46]).

Table 1. Critical void area fraction f_c for site percolation in two-dimensional lattices (after Zallen [46]).

LATTICE	SITE PERCOLATION THRESHOLD p_c^s	FILLING FACTOR v	CRITICAL LACUNITY f_c
Triangular	0.500	0.907	0.45
Square	0.593	0.785	0.47
Honeycomb	0.698	0.605	0.42

In the case of overlapping (intersecting, permeable, soft-core) voids, the problem becomes somewhat more complicated. It is first necessary to determine the probability of overlapping of neighboring voids. The percolation threshold will then coincide with the appearance of an infinite cluster of overlapping voids whose centers need not occupy the nodes of a regular lattice. Obviously, two voids of equal radii r will overlap if the distance between their centers is smaller than $2r$. SHANTE and KIRKPATRICK [53] have shown that the probability that a randomly selected point does not belong to a circular void is equal to e^{-n}, where n is the mean number of circular voids within a distance r from that point. At percolation, the critical value of n becomes $n_c = zp_c^s/4$, where z is the coordination or connectivity number denoting the number of closest nodes. The critical fractional area of voids in a 2D case is (BALBERG [54])

$$f_c = 1 - e^{-B_c/4}, \tag{6.3}$$

where the parameter B_c is the average critical number of circle centers within a given circle (mean number of object intersections). In three-dimensional case, the critical fractional volume for permeable spherical voids becomes

$$f_c = 1 - e^{-B_c/8}. \tag{6.4}$$

Similarly as the critical lacunity (6.2) for hard-core voids, for soft-core voids the critical values of B_c, hence f_c, given in (6.3) and (6.4) manifest a universal behavior. This universality was demonstrated by PIKE and SEAGER [55] in an extensive program of numerical simulations.

Geometrical interpretation of the universal parameter B_c is quite instructive. BALBERG *et al.* [56] have found that

$$
\begin{aligned}
B_c &= N_c\langle A_{\text{ex}}\rangle \qquad \text{(in two dimensions)},\\
B_c &= N_c\langle V_{\text{ex}}\rangle \qquad \text{(in three dimensions)},
\end{aligned}
\tag{6.5}
$$

where N_c is the critical number of defects at percolation, and $\langle V_{\text{ex}}\rangle$ is the so-called mean excluded volume.

The mean excluded volume $\langle V_{\text{ex}}\rangle$ (or area $\langle A_{\text{ex}}\rangle$ in 2D) of an object (A) is enveloped by the locus of points formed by the centers of all surrounding geometrically similar objects (B) which just touch the object (A) without intersecting it. In other words, if a center of an adjacent object (D) is within the excluded volume of a similar object (A), two objects will penetrate each other, Fig. 1. For the circular holes of equal radii shown in Fig. 1, the excluded area is simply $\langle A_{\text{ex}}\rangle = \pi 4r^2$.

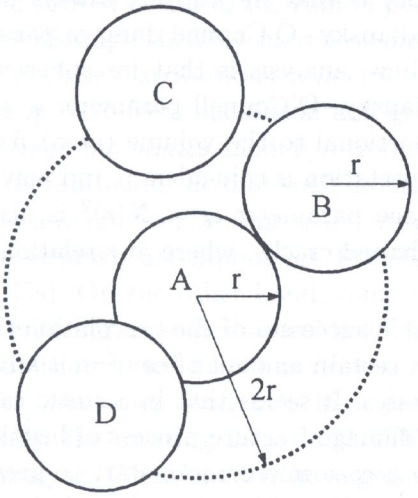

FIG. 1. Excluded area (dotted line) for a circular void A.

In the case of slits, the average number of intersections B_c is, indeed, a dimensional invariant, but the critical crack density parameter $N_c r^2$ is not (ROBINSON [57]). As for disks of constant radius r and vanishing thickness (penny-shaped cracks) uniformly distributed in a homogeneous, elastic material, the critical crack density is $\omega_c = N_c r^3 = 0.182$, whereas the crack intersections density at percolation equals $B_c = N_c\langle V_{\text{ex}}\rangle = \pi^2 N_c r^3 = 1.80$, CHARLAIX [58]. Note that the percolation threshold denotes here the one when an infinite cluster first penetrates a 3D specimen from one side to the opposite one (conductivity percolation threshold). It should not be confused with the second percolation threshold (elastic percolation threshold) at which the specimen looses its integrity and the

secant elastic modulus drops to zero. Naturally, in a two-dimensional system both thresholds coincide. However, in the considered 3D case, the elastic percolation threshold, leading to fragmentation, should occur at a substantially larger density of penny-shaped cracks.

Concluding this section, it seems justified to say that the percolation studies confirm the utility of the Walsh-Budiansky-O'Connell crack density parameter (2.7) in damage modeling, at least for non-intersecting defects. Although the starting points for continuum and percolation theories of brittle damage were quite different, both types of modeling ended up with virtually the same parameter quantifying the evolving material deterioration. For non-intersecting defects, the critical value of this parameter was even proven to be a universal quantity. In other words, upon recognizing that the emergence of an infinite cluster in a two-dimensional case means the final disintegration (fragmentation) of a specimen in a strain-controlled tensile test, a far-reaching conclusion furnished by the percolation theory is that the rupture always happens at the constant value of the Walsh-Budiansky-O'Connell damage parameter. Another conclusion drawn from the above analysis is that for spherical or circular hard-core voids, the Walsh-Budiansky-O'Connell parameter $\omega = N\langle r\rangle^3$ ($\omega = N\langle r\rangle^2$ in 2D) is apparently proportional to the volume (area) fraction of defects, i.e. to the porosity. This interpretation is coincidental and may be misleading, though, because the same damage parameter $\omega = N\langle r\rangle^2$ is also derived for slits, and $\omega = N\langle r\rangle^3$ for penny-shaped cracks, where any relation to material porosity is irrelevant.

Despite unquestionable successes of the percolation theory in the description of critical phenomena, a certain amount of caution is advisable when applying it to model fracture processes. It seems that in a static case, this is *not* a correct model to represent the damage-fracture process of brittle solids. It is a common knowledge that in such a case microcracks start to grow from the pre-existing flaws. The longest and most favorably oriented crack, i.e. the one located perpendicularly to the maximum tensile stress direction, is the first to move provided that its elastic strain energy release rate reaches a critical value. This, however, does not have much in common with the simple bi-modal disorder in the percolation models. Also, the existing percolation models are almost exclusively confined to tensile loading conditions whereas for brittle solids compressive stress states are of primary importance.

On the other hand, the percolation models seem to be more suitable for the description of dynamic fracture processes. Short duration times and high intensity of stress impulses amplify the random character of microcrack nucleation and proliferation. In particular, brittle spall damage, which by its very nature involves random nucleation of defects under the action of tensile stress waves,

offers a promising and yet unexplored field of possible applications of the percolation theory. Some initial efforts in this direction can be found in DIENES [59] and TONKS [60].

7. CLOSURE

Certain conclusions regarding particular spall models have already been drawn in the preceding sections. Here, more general comments will be added and developments of future research will be outlined.

It is now widely accepted that a realistic spall fracture model must quantify in some way the presence and evolution of microcracks or voids within the material. The early models based on the critical stress criterion (spall threshold), and not accounting for the initial damage, turned out to be insufficient. Among the spall models that survived and proved useful in the contemporary fracture dynamics, two main streams can be distinguished: 1) *mesomechanical* models incorporating the number density and size distributions of microdefects in the formulation of rate equations for the microdefects nucleation and growth (SRI models, and alike); 2) *continuum damage mechanics* models introducing a continuum measure for an intrinsically discontinuous field of spall damage (Sandia models, and alike). A step deeper, into a microlevel (atomic scale) of spall processes, although interesting, has not been seriously attempted yet. Possible reasons for that were pointed out by DIENES [34]. On the other hand, some useful information with regard to the constants entering mesomechanical spall models can be furnished by the atomic scale simulations based on the molecular dynamics.

In many spall and fragmentation studies, a high precision in predictions is actually not needed. Thus, the existing meso- and CDM models may provide efficient tools for spall analysis. These models have grown up to the level where they can be used in FEM codes and the obtained predictions of spall damage, time to fracture, size of fragments, etc., are quite satisfactory for engineering purposes. These models will probably get refined as more data is available. However, more sophisticated models require more computing power. Consequently, in order to keep the balance between sophistication and applicability, some models may actually have to be simplified.

For ductile metals in low to moderate shock conditions, the knowledge of the microvoid volume fraction (porosity) $\xi(\mathbf{x}, t)$ seems to be a sufficient prerequisite for the construction of a workable model of spall fracture. In other words, a single damage parameter is expected to perform well here. In high shock conditions, temperature has to be also accounted for since thermomechanical couplings may be significant.

While ductile metallic materials can sustain large compressive stresses without failure, the brittle solids are susceptible to failure both under tensile and compressive stresses, even though the compressive strength of such solids is typically of the order of magnitude higher than the tensile one. In brittle spalling (tension states), it is necessary to account for the distributions of crack sizes and orientations which rules out a single parameter damage model. Under the action of shock waves (compression states), the failure modeling is even more complicated for one has to start with mesomechanical cracking mechanisms that produce local tensile stresses needed for the cracks to grow.

Acknowledgment

This work was supported in part by the Polish State Committee for Scientific Research (KBN) under the grant no. 7TO7A02608. A support from the Deutsche Forschungsgemeinschaft (SFB 298) in the final phase of the project, and the hospitality of the Institute of Mechanics, TU Darmstadt, are appreciated.

References

1. A. Zurek and M.A. Meyers, *Microstructural aspects of dynamic failure*, [in]: High-Pressure Shock Compression of Solids II, L. Davison, D.E. Grady and M. Shahinpoor [Eds.], Springer, 1996.
2. B. Hopkinson, *Scientific papers*, Cambridge University Press, London 1910.
3. J.S. Rinehart, *Some quantitative data bearing on the scabbing of metals under explosive attack*, J. Appl. Phys., **22**, 555–560, 1951.
4. J.S. Rinehart, *Scabbing of metals under explosive attack: Multiple scabbing*, J. Appl. Phys., **23**, 1229–1233, 1952.
5. J.H. Smith, *Three low pressure spall thresholds in copper*, [in]: Dynamic Behavior of Materials, 264–282, ASTM, Philadelphia 1963.
6. F.R. Tuler and B.M. Butcher, *A criterion for the time dependence of dynamic fracture*, Int. J. Fract. Mech., **4**, 431–437, 1968.
7. D.E. Grady and M.E. Kipp, *Dynamic rock fragmentation*, [in]: Fracture Mechanics of Rocks, B.K. Atkinson [Ed.], Academic Press, 429–475, 1987.
8. M.A. Meyers, *Dynamic behavior of materials*, J. Wiley and Sons, New York 1995.
9. J. Eftis, *Constitutive modeling of spall fracture*, [in]: High-Pressure Shock Compression of Solids II, L. Davison, D.E. Grady and M. Shahinpoor [Eds.], Springer, 1996.
10. L. Davison and A.L. Stevens, *Continuum measures of spall damage*, J. Appl. Phys., **43**, 988–994, 1972.
11. L. Davison and A.L. Stevens, *Thermomechanical constitution of spalling elastic bodies*, J. Appl. Phys., **44**, 668–674, 1973.

12. L. DAVISON, A.L. STEVENS and M.E. KIPP, *Theory of spall damage accumulation in ductile metals*, J. Mech. Phys. Solids, **25**, 11–28, 1977.

13. L. SEAMAN, T.W, BARBEE and D.R. CURRAN, *U.S. Air Force Weapons Laboratory Report*, AFWL-TR-71-156, 1971.

14. D.E. GRADY and M.E. KIPP, *Continuum modeling of explosive fracture in oil shale*, Int. J. Rock. Mech. Min. Sci. & Geomech. Abstr., **17**, 147–157, 1980.

15. D.E. GRADY, *Local inertial effects in dynamic fragmentation*, J. Appl. Phys., **53**, 322–325, 1982.

16. D.E. GRADY, *The spall strength of condensed matter*, J. Mech. Phys. Solids, **36**, 353–384, 1988.

17. J.B. WALSH, *The effect of cracks on the compressibility of rocks*, J. Geophys. Res., **70**, 381–389, 1965.

18. J. LEMAITRE and J.-L. CHABOCHE, *Mécanique des Materiaux Solides*, Dunod, Paris 1985.

19. B. BUDIANSKY and R.J. O'CONNELL, *Elastic moduli of cracked solid*, Int. J. Solids Struct., **12**, 81–97, 1976.

20. A.L. GURSON, *Continuum theory of ductile rupture by void nucleation and growth*, J. Engng. Mater. Tech., **99**, 2–15, 1977.

21. V. TVERGAARD and A. NEEDLEMAN, *Analysis of the cup-cone fracture in a round tensile bar*, Acta Metall., **32**, 157–169, 1984.

22. D.E. GRADY, *Spall and fragmentation in high-temperature metals*, [in:] High-Pressure Shock Compression of Solids II, L. DAVISON, D.E. GRADY and M. SHAHINPOOR [Eds.], Springer, 1996.

23. L. SEAMAN, D.R. CURRAN and D.A. SHOCKEY, *Computational models for ductile and brittle fracture*, J. Appl. Phys., **47**, 4814–4826, 1976.

24. D.A. SHOCKEY, D.R. CURRAN, L. SEAMAN, J.T. ROSENBERG and C.F. PETERSEN, *Fragmentation of rock under dynamic loads*, Int. J. Rock Mech. Sci. & Geomech. Abstr., **11**, 303–317, 1974.

25. P. PERZYNA, *Internal state variable description of dynamic fracture of ductile solids*, Int. J. Solids Structures, **22**, 797–818, 1986.

26. D.R. CURRAN and L. SEAMAN, *Simplified models of fracture and fragmentation*, [in]: High-Pressure Shock Compression of Solids II, L. DAVISON, D.E. GRADY and M. SHAHINPOOR [Eds.], Springer, 1996.

27. D.R. CURRAN, L. SEAMAN and D.A. SHOCKEY, *Dynamic failure of solids*, Phys. Reports, **147**, 253–388, 1987.

28. D.R. CURRAN, L. SEAMAN, T. COOPER and D.A. SHOCKEY, Int. J. Impact Engng., **13**, 53–83, 1993.

29. S.J. BLESS and A.M. RAJENDRAN, *Initiation and propagation of damage caused by impact on brittle materials*, [in]: High-Pressure Shock compression of Solids II, L. DAVISON, D.E. GRADY and M. SHAHINPOOR [Eds.], Springer, 1996.

30. A.M. RAJENDRAN, *Modeling of impact behavior of AD85 ceramic under multiaxial loading*, Int. J. Impact Engng., **15**, 749–768, 1994.

31. A.M. RAJENDRAN, M.A. DIETENBERGER and D.J. GROVE, *A void-based failure model to describe spallation*, J. Appl. Phys., **65**, 1521–1527, 1989.

32. C.T. AIMONE, M.A. MEYERS and N. MOJTABAI, [in]: Rock Mechanics in Productivity Design, D.H. DOWDING and M.M SINGH [Eds.], Warrendale, PA, 979, 1984.

33. L.H.L. LOURO and M.A. MEYERS, J. Mater. Sci., **24**, 2516, 1989.

34. H. HORII and S. NEMAT-NASSER, *Brittle failure in compression: splitting, faulting and brittle-ductile transition*, Phil. Trans. Roy. Soc. London, **319**, 337–374, 1986.

35. J.K. DIENES, *A unified theory of flow and fragmentation*, [in]: High-Pressure Shock Compression of Solids II, L. DAVISON, D.E. GRADY and M. SHAHINPOOR [Eds.], Springer, 1996.

36. J.F. KALTHOFF and S. WINKLER, FAILURE MODE TRANSITION AT HIGH RATES OF SHEAR LOADING, [in]: Impact Loading and Dynamic Behavior of Materials, Vol. 1, C.Y. CHIEM *et al.* [Eds.], Informationsgesellschaft Verlag, 1987.

37. J.N. JOHNSON, *Dynamic fracture and spallation in ductile solids*, J. Appl. Phys., **53**, 2812–2825, 1981.

38. J. EFTIS and J.A. NEMES, *An evolution equation for the void volume growth rate in a viscoplastic-damage constitutive model*, Int. J. Plasticity, **7**, 275–293, 1991.

39. J.R. KLEPACZKO, *Dynamic crack initiation: some experimental methods and modelling*, [in]: Crack Dynamics in Metallic Materials, J.R. KLEPACZKO [Ed.], Springer, 1990.

40. H. DENG and S. NEMAT-NASSER, *Dynamic damage evolution in brittle solids*, Mech. Mater., **14**, 83–103, 1992.

41. M.A. MEYERS, Mech. Mater., **4**, 387, 1985.

42. G.P. CHEREPANOV, *Mechanics of brittle fracture*, McGraw-Hill, 1979.

43. V.N. NIKOLAEVSKI, *Limit velocity of fracture front and dynamic strength of brittle solids*, Int. J. Engng. Sci., **19**, 41–56, 1981.

44. Y.L. ZILBERBRAND, N.A. ZLATIN, A.A KOZUSHKO, V.I. POLOZENKO, G.S. PUGACHEV and A.B. SINANI, *Mechanism of interaction of a plastic striker with a brittle solid*, Sov. Phys.-Tech. Phys., **34**, 1123–1124, 1989.

45. G.I. KANEL, S.V. RASORENOV and V.E. FORTOV, *The failure waves and spallations in homogeneous brittle materials*, [in]: Shock Compression of Condensed Matter, Elsevier, 1992.

46. R. ZALLEN, *The physics of amorphous bodies*, J. Wiley and Sons, New York 1983.

47. D. STAUFFER, *Introduciton to percolation theory*, Taylor & Francis, London, UK 1985.

48. H.J. HERRMANN and S. ROUX, *Statistical models for the fracture of disordered media*, North-Holland, The Netherlands 1990.

49. M. BASISTA and D. KRAJCINOVIC, *Brittle deformation of disordered solids*, Composites Engng., **1**, 103–112, 1991.

50. D. KRAJCINOVIC, M. BASISTA and D. SUMARAC, *Basic principles of damage mechanics*, [in]: Damage Mechanics of Composite Materials, R. TALREJA [Ed.], Elsevier, 1994.

51. D. KRAJCINOVIC, *Damage mechanics*, Elsevier, The Netherlands 1996.

52. H. SCHER and R. ZALLEN, *Critical density in percolation processes*, J. Chem. Phys., **53**, 3759–3761, 1970.

53. V.K.S. SHANTE and S. KIRKPATRICK, *An introduction to percolation theory*, Adv. Phys., **20**, 325–357, 1971.

54. I. BALBERG, *Recent developments in continuum percolation*, Phil. Mag. **B56**, 991–1003, 1987.

55. G.E. PIKE and C.H. SEAGER, *Percolation and conductivity: A computer study*, Phys. Rev B, **10**, 1421–1446, 1974.

56. I. BALBERG, C.H. ANDERSON, S. ALEXANDER and N. WAGNER, *Excluded volume and its relation to the onset of percolation*, Phys. Rev. B, **30**, 3933–3943, 1984.

57. P.C. ROBINSON, *Numerical calculations of critical densities for lines and planes*, J. Phys. A, **17**, 2823–2830, 1984.

58. E. CHARLAIX, *Percolation thresholds of a random array of discs: A numerical simulation*, J. Phys. A, **19**, L533–L536, 1986.

59. J.K. DIENES, *Permeability, percolation, and statistical crack mechanics*, [in:] Issues on Rock Mechanics, R.E. GOODMAN and F.E. HEUZE [Eds.], Proc. 23rd Symp. on Rock Mech., Berkeley, CA., 1982.

60. D.L. TONKS, *Disorder, percolation and wave propagation effects in ductile fracture*, [in]: High-Pressure Shock Compression of Solids II, L. DAVISON, D.E. GRADY and M. SHAHINPOOR [Eds.], Springer, 1996.

POLISH ACADEMY OF SCIENCES
INSTITUTE OF FUNDAMENTAL TECHNOLOGICAL RESEARCH.
e-mail:mbasista@ippt.gov.pl

Received November 14, 1997.